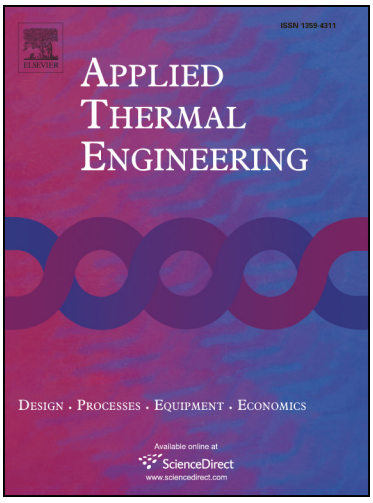

Simulation models for tankless gas water heaters

André F. Quintã, Jorge A.F. Ferreira, António Ramos, Nelson A.D. Martins, Vítor A.F. Costa

PII: S1359-4311(18)34723-9
DOI: https://doi.org/10.1016/j.applthermaleng.2018.11.095
Reference: ATE 12976

To appear in: *Applied Thermal Engineering*

Received Date: 31 July 2018
Revised Date: 5 November 2018
Accepted Date: 23 November 2018

Please cite this article as: A.F. Quintã, J.A.F. Ferreira, A. Ramos, N.A.D. Martins, V.A.F. Costa, Simulation models for tankless gas water heaters, *Applied Thermal Engineering* (2018), doi: https://doi.org/10.1016/j.applthermaleng.2018.11.095

Simulation models for tankless gas water heaters

André F. Quintã [a], Jorge A. F. Ferreira [a], António Ramos [a], Nelson A. D. Martins [a], Vítor A. F. Costa [a]
[a] Departamento de Engenharia Mecânica, Universidade de Aveiro, Campus Universitário de Santiago, 3810-193 Aveiro Portugal

highlights

- Models for individual components of tankless gas water heaters are developed.
- Experiments are conducted to determine calibration parameters for heat cell model.
- Simulation for different configurations and scenarios are conducted.

Abstract

There is a growing concern about to the scarceness of natural resources and the emissions problematic. Water heating is a relevant part of a household's energy use, and tankless gas water heaters (TGWH) are widely used. There are design and engineering challenges to develop more efficient devices, with lower emissions of pollutant gases and providing comfort improvements from the user point of view.

The main objective of the present work is to provide mathematical models to evaluate and support the development of different TGWH configurations. By simulation, different hardware configurations and advanced control strategies can be tested and optimized regarding energy saving, reducing of harmful environmental emissions and increase of comfort indices by reducing temperature undershoots and overshoots.

The TGWH individual components are modelled, laboratory tests are performed and the heat cell is parametrized with experimental data. Configurations with and without bypass function are performed for several water flow rates and setpoint temperature patterns in open loop and with feed-forward control.

Keywords: Tankless gas water heaters, Gas fired, Instantaneous heating, Domestic hot water, Modelling, Simulation

Nomenclature

A	[m^2]	Area	$\dot{q}$	[$m^3.s^{-1}$]	Volumetric flow rate
c_p	[$J.kg^{-1}.ºC^{-1}$]	Constant pressure specific heat	$\dot{Q}$	[W]	Heat transfer rate
C_d	[]	Discharge coefficient	R	[m]	Radius
g	[$m^3.Pa^{-1}.s^{-1}$]	Orifice conductance	Re	[]	Reynolds number
h	[$W.m^{-2}.ºC^{-1}$]	Convection heat transfer coefficient	t	[s]	Time
k	[$W.C^{-1}.m^{-1}$]	Thermal conductivity	T	[°C]	Temperature
L	[m]	Length	U	[$W.m^{-2}.ºC^{-1}$]	Overall heat transfer coefficient
m	[kg]	Mass	V	[m^3]	Volume
$\dot{m}$	[$kg.s^{-1}$]	Mass flow rate	β	[Pa]	Bulk modulus
P	[Pa]	Pressure	ρ	[kg m^{-3}]	Density

1. Introduction

Currently, there is a growing awareness and concern with the scarceness of natural resources, associated with the noticeable increase in energy consumption and harmful emissions, causing adverse effects to the environment and society.

Water heating represents a significative part of the total buildings energy consumption, domestic hot water production accounting for approximately 18% of total energy consumption in the residential sector in the USA [1] and 14,5% in the European Union [2].

The European Union defined energy policies to meet the challenges related to climate changes, security of supply, and competitiveness with new energy labelling and ecodesign requirements for heaters and water heaters. Ecodesign requirements are mandatory for all heater manufacturers and suppliers wishing to sell their products in the EU. The regulations set requirements on energy efficiency, nitrogen oxide emission levels, volume for storage water heaters, and heat losses from hot water storage tanks, [3], bringing new challenges to the manufactures.

Gas fired water heaters are widely used for domestic hot water production. TGWH is one of the more popular choices when replacing tank based heaters. TGWH is the most efficient conventional method of generating heat from natural gas in a domestic hot water application, [4].

One of the most relevant drawbacks of TGWH is the difficulty to maintain stability of the outlet hot water temperature as changes in water flow rate can be very fast and unpredictable, the system has its own thermal inertia, the temperature changes travel at the water flow velocity, and the thermal and fluid dynamics are linked and inherently nonlinear, [5]. Some of the more advanced TGWH systems have gas modulation, feedback flow rate and temperature sensors and electronic control units with PID controllers. However, the evolution for faster and more robust control persist. One of the most promissory answers is model predictive control (MPC), as already demonstrated by [6] and [7], for electric tankless water heaters.

The TGWH temperature stability problem is shown in Figure 1, where experimental data are presented. Hot water temperature overshoots and undershoots are observed for water flow rate quick changes on an appliance with feedback control and a bypass circuit.

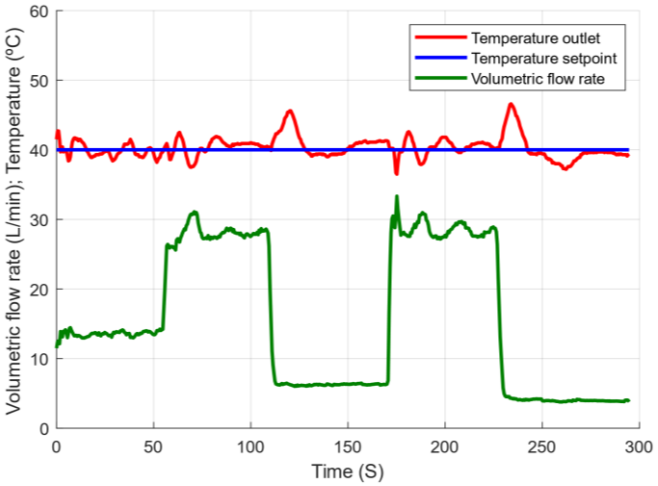

Figure 1: Experimental data for TGWH hot water exit temperature.

There are many gas water heater simulation models developed by the scientific community. The earlier models like TANK, WATSIM and HEATER focus on tank temperature spatial distribution and are unable to model tankless instantaneous heaters. Many other models have been developed based on TRNSYS [8] for specific studies such as the integration with renewable energy using TGWH as an auxiliary energy source [9] or parametric cost-effective analysis of the most common water heating technologies [10].

A preliminary model for a TGWH, based on TRNSYS, is presented by [11], and consists of a single lumped node for the heat exchanger and water mass, with coupling to environment heat loss and gas input. The model is used to efficiency calculation with standard test and a more realistic draw pattern.

Addition of a small external storage tank was considered in an attempt to eliminate minimum flow rate and hot water delay.
Simulation models of Tank and Tankless non-condensing water heaters were also developed [12]. Those were implemented in Modelica language using Dymola development studio and designed to be included in the LBNL Buildings Library, a collection of simulation models for residential hot water systems. The model for the tankless water heaters as two components, the heat exchanger and a PID controller, and experimental data were compared against simulation results for a specific appliance.
Johnson and Beausoleil-Morrison [13] developed a model to describe the energy input-output relationship based on analytical solutions to TWH modelled with a lumped heat capacity. A first-order step response model, combined with an initial impulse model, was proposed and calibrated with experimental data to represent energy performance of condensing TGWH.
The TGWH models identified in the literature are mainly based on energy balance with a focus on efficiency performance, for applications on domestic hot water systems, considering the appliance as a global model, without detailed fluid and thermal models of individual components, such as internal pipes and water valves. Therefore, these models are unsatisfactory to support the evaluations of innovative component configurations and development of advanced predictive control strategies.
Due to the extensive use of TGWH for domestic water heating, it is extremely relevant to conduct research for improvements to increase energy and water savings, emissions efficiency and user comfort. These are the main goals of one of the development lines of the more enlarged project Smart Green Homes.

2. Modeling GWH components

Some basic configurations of TGWH have relatively simple gas and water circuits, with a direct connection from the water inlet to a manual flow valve, then to the heat exchanger and finally to the outlet. However, more complex appliances, with electronic control, may have electric actuated flow control valves, bypass water circuits or reservoirs for implementation of temperature control strategies, as schematically presented in Figure 2.

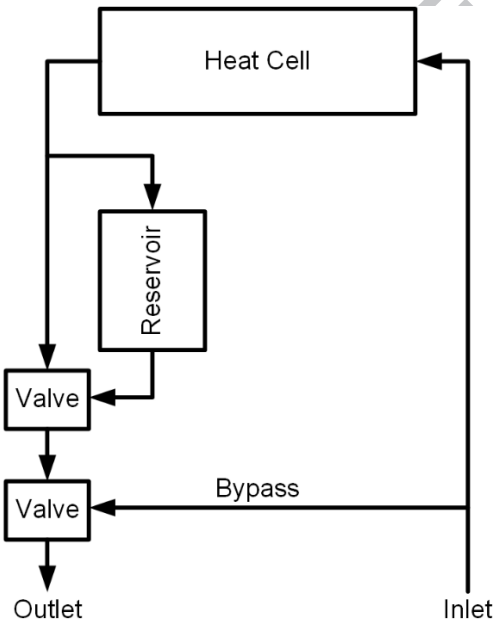

Figure 2: Schematic of a TGWH with reservoir and bypass circuit.

To develop and simulate new configurations of TGWH internal connections, using different components, with different parameters and connected in different ways, a modeling methodology was established in which individual parts of each internal component are modelled, describing thermal, fluid and mechanical dynamics. Then models of each component are interconnected, creating TGWH devices with different hardware configurations that could be parameterized differently.
A lumped space approach was used to model individual components. The lumped system analysis was preferred over distributed analysis, considered through a finite element or finite difference methods, in order to meet the requirements for implementation of predictive control algorithms in computationally limited embedded systems.
The mathematical models result from the application of physical laws that describe, with small deviations, the dynamics of the system. For the heat cell, a semi-empirical model was used.
The individual components considered for modelling are a pipe, split, junction, reservoir, valves and heat cell. Each component is modelled considering a control volume, for which mass and energy conservation equations, are established. The thermal component is detached from the fluidic part.
The fluidic component describes pressure and fluid flow dynamics, starting from the mass conservation law applied to a control volume,

$$\frac{dm_{CV}}{dt} = \sum_{in} \dot{m} - \sum_{out} \dot{m} \tag{1}$$

The thermal dynamics is based on the energy conservation equation for the control volume under analysis. Only the internal energy variations are considered, the kinetic and gravitational potential energy variations are assumed negligible and mass inside each control volume is considered to be constant. The energy conservation equation for a control volume comes,

$$mc_p \frac{dT}{dt} = \dot{Q} + \sum_{in} \dot{m} c_p T - \sum_{out} \dot{m} c_p T \tag{2}$$

From the mass conservation equation for a constant volume, the pressure dependence on the volumetric flow rates can be set by the equation,

$$\frac{dP}{dt} = \frac{\beta}{V}(\dot{q}_{in} - \dot{q}_{out}) \tag{3}$$

where β is the bulk modulus defined as

$$\beta^{-1} = -\frac{1}{V}\left(\frac{\partial \mathrm{V}}{\partial \mathrm{P}}\right)_T \tag{4}$$

The Reynolds number is used to determine the regime of water flow in each component. For turbulent flow, the water volumetric flow rate through an orifice is expressed by

$$\dot{q} = sign(\Delta P) C_d A_0 \sqrt{\frac{2}{\rho}\Delta P} \tag{5}$$

where A_0 is the orifice area and C_d the discharge coefficient.
For laminar flow, the water flow rate is expressed considering a hydraulic conductance, as

$$\dot{q} = \mathrm{g}\Delta P \tag{6}$$

2.1. Pipe model

For the internal water pipe model, the heat losses from the water to the outside environment are described by the heat transfer through the walls of the tube, first by convection to the inner wall of the tube, then by conduction in the tube wall and then by convection from the outer wall of the tube to the environment.
The overall heat transfer coefficient U_i, based on the inner radius of the tube, is obtained as

$$\mathrm{U}_i = \frac{1}{\frac{1}{h_i} + \frac{R_i}{k_m} ln\left(\frac{R_e}{R_i}\right) + \frac{R_i}{R_e}\frac{1}{h_e}} \tag{7}$$

For the convective heat transfer on the outside of the pipe, the conditions remain essentially constant, and the convection heat transfer coefficient h_e has been considered approximately constant. However, this is not valid for the forced convection heat transfer coefficient inside the pipe, h_i, as the water flow conditions vary significantly. The internal convective heat transfer coefficient was calculated, for a turbulent flow, from the Nusselt number Nu determined by the Gnielinski correlation[14], and the friction factor determined by the Petukhov correlation [15].
Considering the heat losses to the environment, the pipe equation energy conservation is,

$$\frac{dT_i}{dt} = \frac{-\mathrm{U}2\pi R_i L(T_i - T_{amb}) + \dot{m}c_{p,w}(T_{\mathrm{in}} - T_i)}{\pi L\left[\rho_w {R_i}^2 c_{p,w} + \rho_m({R_e}^2 - {R_i}^2)c_{p,m}\left(1 - \frac{U}{h_i}\right)\right]} \quad (8)$$

The adopted lumped system analysis doesn't consider the temperature variation inside the pipe. The time delay of changes in the outlet temperature due to the water flow rate is determined by the average water velocity; regarding the definition of mass flow rate, for a circular section pipe, it is

$$\Delta t = \frac{L\rho\pi {R_i}^2}{\dot{m}} \quad (9)$$

A spatial temperature distribution, if needed, can be achieved by interconnecting several pipe segments with a small length.
The internal pipe water pressure evolution is obtained from Equation 3, and inlet water flow rate is obtained from Equation 6.

2.2. Split and junction models

The simpler TGWH configurations have linear water circuits, with components connected in series, from the inlet to the outlet; however, in some more complex configurations such as bypass or internal reservoir, T type pipe connections are used to divide or combine water circuits.
For a water circuit split, a T type pipe is modelled with one inlet and two or more outlets ports. The inlet flow rates are determined for laminar regime from Equation 6 and the pressure and temperature dynamics are described by mass and energy equations.

$$\frac{dP}{dt} = \frac{\beta}{V}(\dot{q}_{in} - \dot{q}_{out1} - \dot{q}_{out2}) \quad (10)$$

$$\frac{dT}{dt} = \frac{1}{m}(\dot{m}_{in}T_{in} - \dot{m}_{out1}\mathrm{T} - \dot{m}_{out2}T) \quad (11)$$

A similar approach is used to establish the equations for a T type pipe model of a junction that mixes water circuits and has two or more inlets and one outlet ports.

2.3. Reservoir model

Some strategies to improve the TGWH performance are based on the thermal inertia of an internal small water reservoir. A small tank is normally used in gas water heaters to reduce the magnitude of undershoots and overshoots on the outlet hot water temperature, and not for hot water (energy) storage, and the system continues being considered a TGWH [5].
The reservoir is modelled as a stratified cylindrical tank constructed as a sequence of lumped model slices as schematically represented in Figure 3. In each slice, the temperature and pressure are assumed to be uniform, and the slices are interconnected in sequence creating a spatial temperature variation.

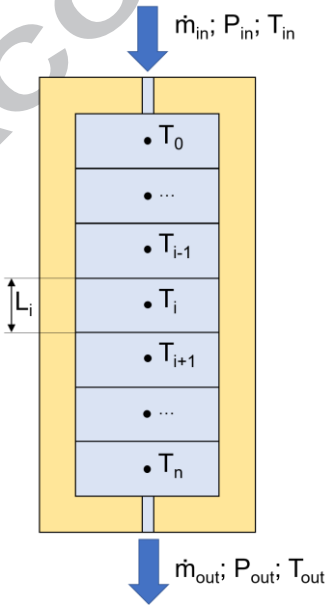

Figure 3: Schematic of the accumulation reservoir slices model.

The internal water pressure is obtained from Equation 3, and the inlet water flow rate is obtained from Equation 6. Heat transfer from the reservoir to the surrounding environment is modelled in a similar way as in the pipe model. Additionally, the heat transfer by water conduction between adjacent slices is described by the Fourier's Law. The thermal dynamics is defined by the energy conservation equation for each slice.

$$mc_{p,w}\frac{dT_i}{dt} = -U_iA_i(T_i - T_{amb}) + kA_c\frac{(T_{\mathrm{i+1}} - T_i)}{L_i} - kA_c\frac{(T_{\mathrm{i}} - T_{i-1})}{L_i} + \dot{m}c_{p,w}(T_{\mathrm{i-1}} - T_i) \quad (12)$$

A_i is the external surface area of the slice *i* and for the bottom and top slices, the area also includes the corresponding bottom or top flat surfaces. In the outer limit bottom and top slices, the water conductive heat transfer is null.

2.4. Valve model

For a two-way proportional flow control valve, the orifice area *A* is determined by the spool position *x* and the radius *R* of the circular water inlet.

$$A = R^2 cos^{-1}\left(\frac{R - x}{R}\right) - (R - x)\sqrt{2Rx - x^2} \quad (13)$$

The flow regime the valve orifice is turbulent and modelled by Equation 5.
The thermal component is defined by the energy conservation equation and the fluidic component by the mass conservation equation in the form of Equation 3 for the control volume of a valve with one inlet and one outlet.
Likewise, a three-way proportional flow control valve is also modelled, following the same methodology. The three-way valve combines water from two inlets, with areas defined by the spool position *x*, to one outlet where the temperature of the mixed water is defined by the energy balance equation as

$$\frac{dT}{dt} = \frac{1}{m}(\dot{m}_{in1}T_{in1} + \dot{m}_{in2}\mathrm{T}_{in2} - \dot{m}_{out}T) \quad (14)$$

Heat losses from the valves to the environment are not considered essential due to their small dimensions (small heat transfer surface area).

2.5. Heat cell model

The heat cell embraces the gas combustion burner and the transfer of energy to the water in the heat exchanger with condensation of water in the flue gases. For the heat cell, assuming that the water and metal (copper alloy) are at a similar temperature and the fluid density variations are negligible, the water temperature at the exit can be expressed by setting the energy conservation equation for a control volume as

$$\frac{dT}{dt} = \frac{1}{m_w c_{p,w} + m_m c_{p,m}}\left(\dot{Q} + \dot{m}_{in}c_{p,w}(T_{in} - T)\right) \quad (15)$$

The heating power $\dot{Q}$ is defined by the flow of air gas mixture, controlled by a gas valve and atmospheric or fan forced air inlet, considering a heating efficiency η.
Such as in the pipe model, water temperature time delay is considered as a function of water average velocity and pipe section.
The fluidic component is described by the continuity equation in the form of Equation 3, and by Equation 5 for the turbulent flow regime.
The heat cell involves processes of greater complexity associated with combustion. As a semi-empirical model has been designed it requires a parametrization using experimental results, to reasonably reproduce the static and dynamic relationship between the water flow rate, the temperature and the thermal power delivered to the heating cell and the temperature of the water at the exit of the heat cell.

2.6. Heat cell model parametrization

Some processes that occur inside the heat cell have high complexity, such as combustion, heat transfer and condensation. In order to maintain the model's complexity within the limits to be used to implement new control methodologies, these processes were empirically modelled and parametrized using laboratory experimental data. A time delay for the thermal power delivery and temperature increments at the heat cell inlet and outlet are considered.

An experimental infrastructure, shown in Figure 4, was developed in the scope of the Smart Green Homes project. This platform is prepared for tests with two parallel TGWH with water supply, condensation waste pipe, consumer water circuit, propane gas supply, electrical connections and flue exhaust gases.

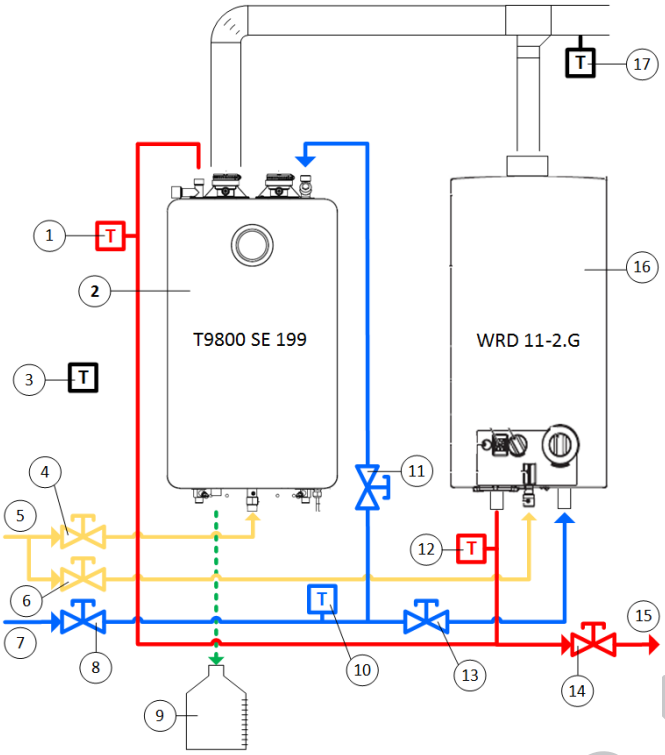

1 - Thermocouple, water outlet A temp.
2 - Appliance A (condensing)
3 - Thermocouple, air temperature
4 - Valve, gas inlet A
5 - Gas connection (propane)
6 - Valve, gas inlet B
7 - Cold water connection
8 - Valve, water inlet
9 - Condensate discharge
10 - Thermocouple, water inlet temp.
11 - Valve, water inlet A
12 - Thermocouple, water outlet B temp.
13 - Valve, water inlet B
14 - Valve, hot water outlet
15 - Hot water connection
16 - Appliance B (non condensing)
17 - Thermocouple, flue gases temp.

Figure 4: Schematic of the experimental set up.

For the model's parametrization, a Bosch Greentherm T9800 SE 199 TGWH was selected. This residential and commercial TGWH condensation model as a thermal power of 58.3 kW, with 99% thermal efficiency, modulating gas and water valves, a bypass circuit and burner power segmentation. The experimental parametrization was focused on the heat cell.

For the heat cell characterization tests, no external instrumentation was used; instead, by communication with the TGWH Electronic Control Unit (ECU), the appliance internal sensors and actuators values where accessed and recorded.

The thermostatic control was disabled, the bypass valve forced in the closed state, and the water restrictor valve was fully open.

For analysis of the heat cell in an open loop in steady-state regime, tests were performed for different values of thermal power and hot water flow rate. The inlet and outlet water temperatures were recorded, as summarized in Table 1 and represented in Figure 5.

The inlet temperature was approximately constant with an average value of 19.4°C. All combinations of power and water flow rate were performed, except when a lower water flow rate combined with a high thermal power lead to temperatures higher than the appliance safety limit.

For the parametrization of the semi-empirical heat cell model, steady-state and transient simulations were performed and matched with experimental data.

Steady-state simulations were performed to parametrize the temperature increments at the heat cell inlet and outlet. Simulations were performed for the same inputs as used in experimental open loop tests, namely inlet water temperature, hot water flow rate and thermal power (Table 1). For each set of inputs, a set of simulations was performed for a vector of temperature increments, and calculations of root mean square error (RMSE) were done to measure the difference between the experimental and simulation outlet water temperature values. The heat cell temperature increments were selected from the minimum RMSE deviation.

Table 1: Average heat cell outlet water temperature (open loop tests).

		Outlet water temperature (°C)				
		Hot water flow (L/min)				
		5	10	15	20	25
Burner Power (kW)	10.0	48.3	34.2	29.2	26.8	25.3
	20.0	77.1	47.7	39.1	34.1	31.0
	30.0		64.0	47.9	41.3	36.2
	40.0		77.8	57.5	48.2	42.1
	50.0			69.3	56.6	48.1
	58.3			78.3	63.6	53.7

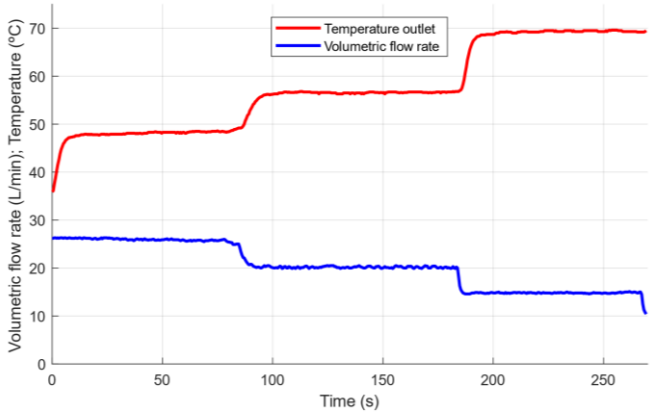

Figure 5: Experimental data the for the heat cell outlet temperature and water flow rate.

The time delay for the thermal power delivery was used for the heat cell model parametrization in transient regime. Experimental tests were performed with constant inlet temperature for several thermal power values with fast changes in the hot water flow rate. The time delay parameter was empirically adjusted to match the experimentally measured temperature with the model predicted outlet temperature response.

3. Simulations

The individual component models were implemented separately in the MATLAB/Simulink platform in a way that different configurations and scenarios can be easily created and simulated.

By connecting components models, two different TGWH configurations were modelled and used in simulations, with and without bypass circuit. The connections between the component model's links temperature, pressure and flow rate values. The temperature and pressure values are transported from upstream to downstream blocks, the inlet flow rate is calculated in each block and transported to the upstream block as the corresponding outlet flow rate through an input as represented in Figure 6 and Figure 7.

The Bosch Greentherm T9800 SE 199 TGWH was modelled and used for simulations in different scenarios. The water circuit configuration of this appliance comprises a bypass circuit to the heat cell with T type pipes for water division and junction and a two-way proportional flow control valve. Two-way valves are also present at the heat cell inlet to enable flow restriction control strategies, and at the hot water, outlet to implement different water flow rate patterns as represented in Figure 8. The pipe model was used to implement hot water circuits; for pipes where cold water circulates the heat transfer for ambient was assumed negligible.

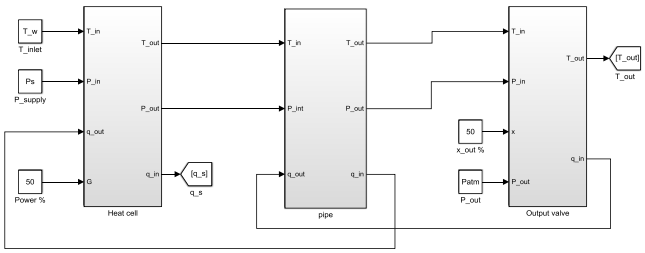

Figure 6: Simulink blocks of TGWH model without bypass.

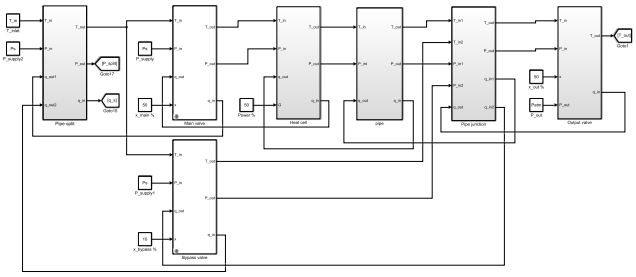

Figure 7: Simulink blocks of TGWH model with bypass.

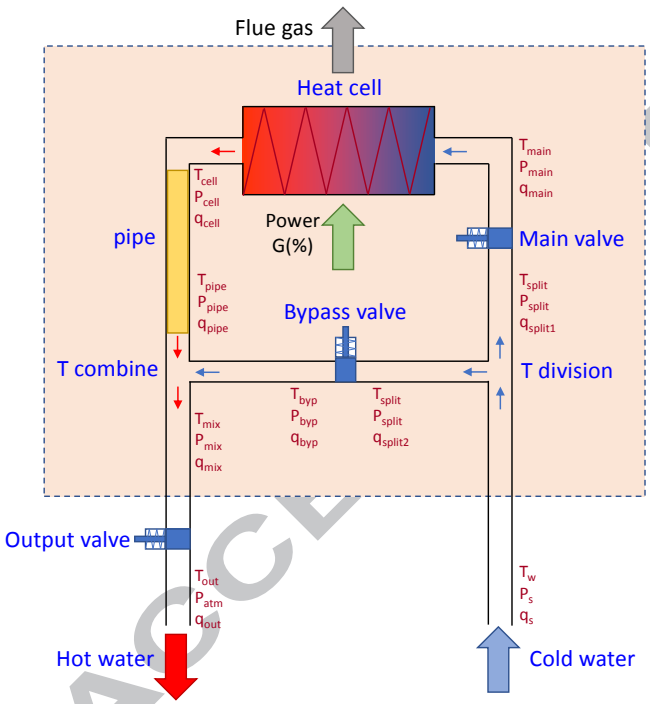

Figure 8: Schematic of TGWH bypass configuration.

The bypass circuit and valve are used to improve the temperature stabilization and minimize temperature overshoots or undershoots. The water leaving the heat cell is defined to be slightly hotter than the required outlet set point and mixed with cold water from the bypass, obtaining a temperature buffer and thus allowing a faster response.

Simulations with TGWH model were performed in open loop and in thermostatic control mode. For open loop simulations, the appliance thermostatic control was disabled, and thermal power was defined as constant for each test, with several water flow rate patterns imposed at the output valve.

In order to assess whether the developed models are suitable for use in the development and testing of innovative control strategies, some closed-loop simulations with a combined feedforward and PID control were also performed. A model was developed for implementing thermal power control as schematically represented in Figure 9.

The feed-forward component is based on the heat exchanger energy balance equation in order to calculate the predicted power needed to heat water from the inlet temperature to the required setpoint temperature in steady-state conditions, for the measured water flow rate, that is

$$\dot{Q}_{FF} = \dot{m}_{in} c_{p,w} (T_{set} - T_{in}) \quad (16)$$

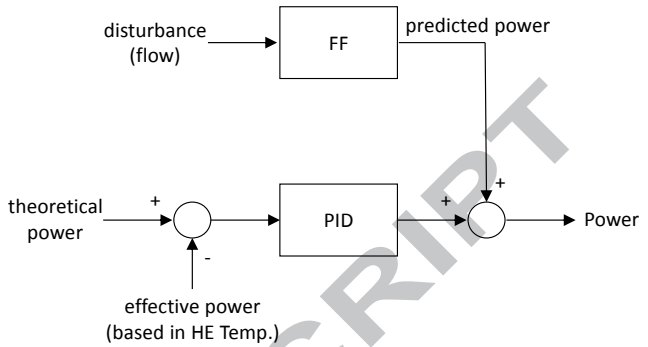

Figure 9: Schematic of the combined feed-forward feedback controller.

For the PID component, the feedback power is calculated based on the measured heat cell outlet temperature. The PID parameters are empirically adjusted and not fully optimized.

4. Results and discussion

A separate set of laboratory tests was performed, in order to collect experimental data, different from the data used for calibration purposes, for model validation purposes. To evaluate the model's performance, several simulations were performed with different configurations and scenarios, and the predicted values were compared to the measured data.

For heat cell characterization, simulations tests were performed with constant inputs for the inlet temperature, water flow rate and thermal power. After stabilization, the average outlet water temperature was recorded. A script was used to perform a set of simulations for combinations of water flow rate and thermal power and compute the colourmap of Figure 10, which presents a fast and simple overview of the behaviour of the heat cell in the steady-state regime.

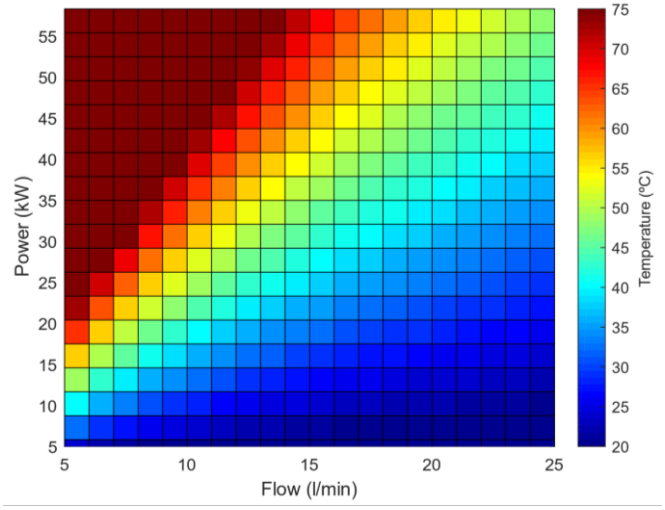

Figure 10: Colourmap for the heat cell outlet water temperature in steady-state conditions.

The calibration data were also compared with simulated constant power curves in Figure 11. A minor dependence of error on the power inlet is observed, which increases for lower and higher power limits.

Simulation tests were performed to estimate the effect of inlet water temperature variations. For a fixed water flow rate of 10 L/min and a thermal power of 23.3 kW, the heat cell outlet water temperature is obtained by simulation with monthly average inlet water temperature in the city of London obtained from the RETScreen Software. The inlet and estimated outlet water temperatures are presented in Figure 12. For inlet water temperature with a

minimum of 9.4 ºC and a maximum of 14.1 ºC, the predicted outlet temperatures are 43.8 ºC and 48.5 ºC respectively.

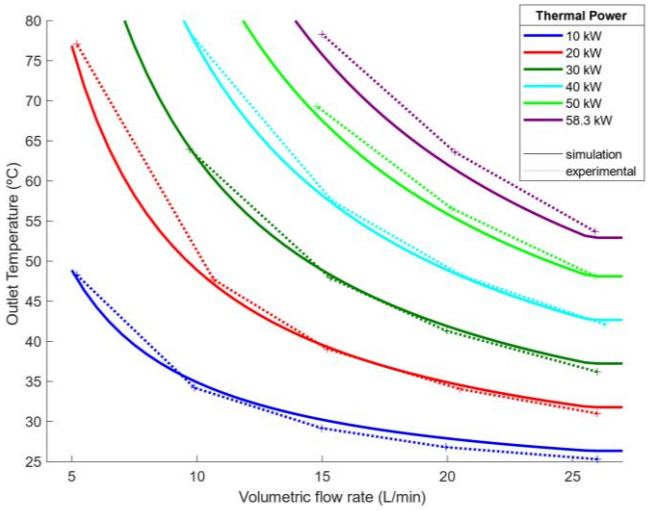

Figure 11: Experimental and simulated heat cell outlet temperature, in steady-state conditions.

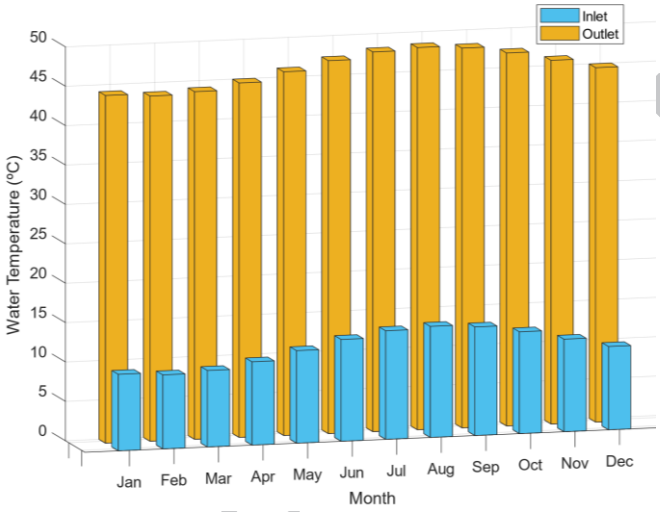

Figure 12: Simulated heat cell outlet water temperature for one-year inlet water temperature variations in London.

The heat cell model performance in transient regime was evaluated by simulation tests with step flow variations and constant thermal power. The predicted response was compared with experimental data in open loop, with the appliance thermostatic control disabled.

Figure 13 presents the simulated and experimental values for a near step flow rate decrease followed by a fast increase after stabilization. Here the experimental data (inlet temperature, input thermal power and water flow rate) were used as model inputs. For a fixed thermal power of 24.4 kW, and inlet temperature of 19.4 °C, the water flow rate presents a fast drop from 25.6 L/min to 8.1 L/min at instant 8 s and a fast rise to 25.8 L/min at instant 46 s. A good overall match is observed with a small delay from the predicted response; a maximum instantaneous difference of 1.7 °C was measured at flow rate decrease and of 1.3 °C at a flow rate increase.

A test with a more demanding sequence of different flow rate sudden changes was also made. The experimental and simulated outlet water temperatures are presented in Figure 14 with a very good fit. A maximum difference of 1.56 °C is observed at instant 22.75 s after a flow rate reduction from 20 L/min to 8 L/min. The mean absolute temperature difference is of 0.32 °C.

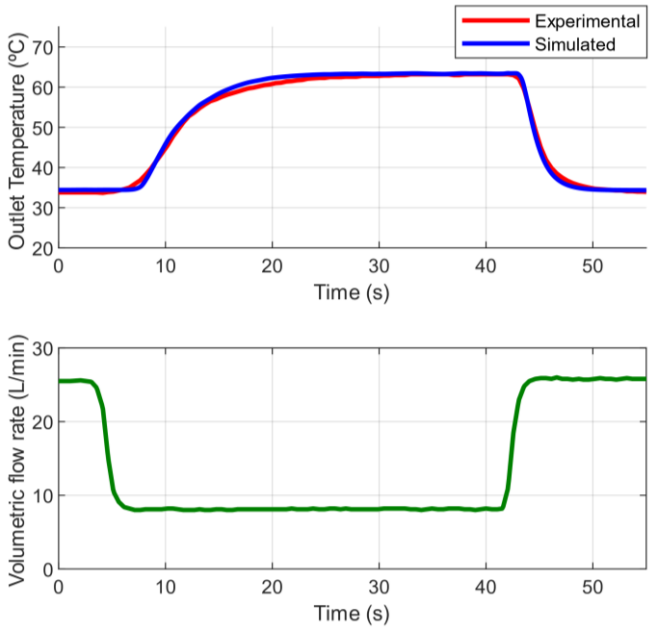

Figure 13: Experimental and simulated heat cell outlet temperature response to a water flow rate step.

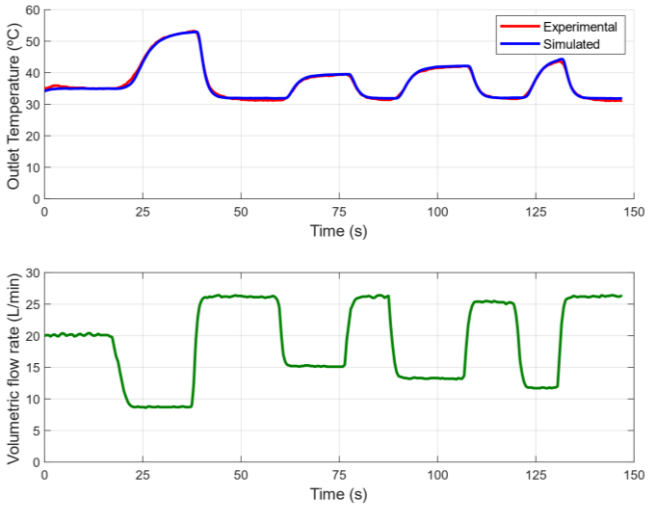

Figure 14: Experimental and simulated heat cell outlet temperature (sequence of flow rate sudden changes).

The model response to thermal power was also evaluated by applying a sequence of step changes on this parameter. Experimental and simulated heat cell outlet water temperature is compared in Figure 15. For this test, the water flow rate has a constant value of 12 L/min. Experimental values were defined as simulation inputs and the thermal power was defined by changing a setpoint parameter in the appliance ECU, the air-gas mixture being automatically adjusted by the appliance power control strategy. A satisfying match between experimental and simulated results is observed, with just a small delay.

One of the main motivations for simulation models is the need to predict the behaviour of unmeasured system variables. For the previous simulation with flow rate step scenario, Figure 16 presents the simulated values for the heat cell water temperature, water pressure and flow rate.

The appliance selected for experimental tests and simulation has a reasonable temperature control response for water flow rate changes, mainly due to the active bypass circuit; however, more economic appliances don't have bypass circuits. Figure 17 presents experimental simulations performed with the same appliance but with the bypass valve disabled for a sequence of several fast water flow rate changes. In this case, significative temperature instability is observed, with a measured temperature overshoot peak of 27 °C.

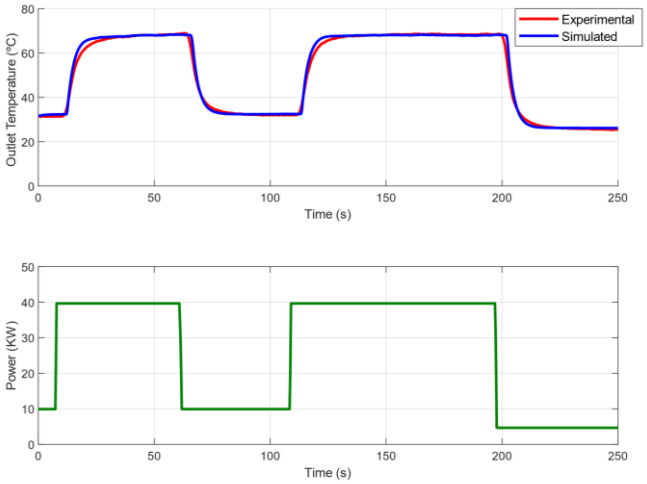

Figure 15: Experimental and simulated heat cell outlet temperature for a power step response.

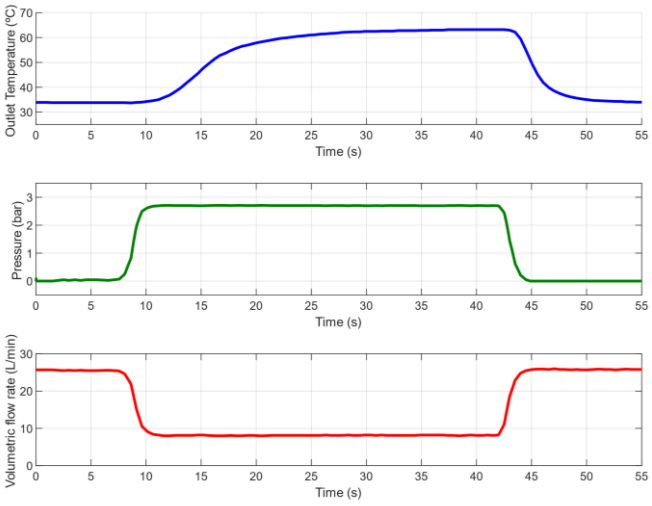

Figure 16: Simulated heat cell water temperature, pressure and flow rate.

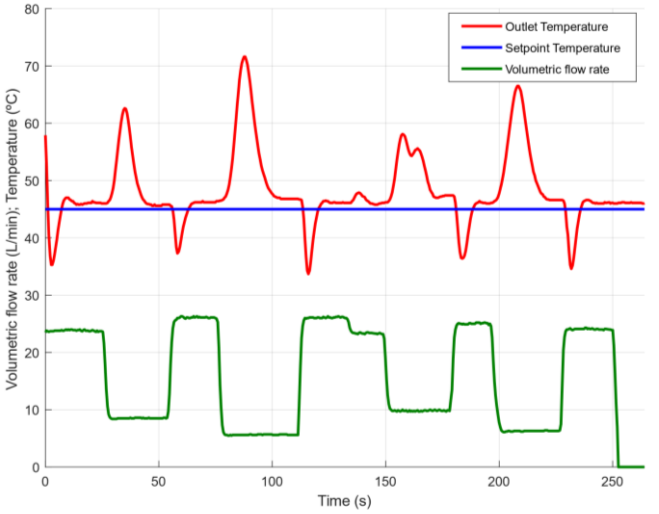

Figure 17: TGWH experimental temperature values, bypass disabled.

The TGWH thermostatic control is implemented by a combined feedforward and PID control model that was evaluated by simulations in several scenarios. Figure 18 presents simulated power and outlet temperature response to step changes in the water flow rate, with and without bypass circuit. The outlet temperature stability is accomplished; nevertheless, some temperature overshoots and undershoots are noticed. The temperature overshoot occurring for the simulation without bypass circuit in the situation of a water flow rate decrease at instant 60 s is almost absent when bypass circuit is considered, and cold inlet water is mixed with the overheated water from the heat cell. However, the control with bypass circuit is unable to deal with fast water flow rate increase, and temperature undershoot is visible at instant 120 s. A small water reservoir may be considered to improve control performance in this case and prevent undershoot occurrence.

5. Conclusion

In the present work, TGWH models were developed, parametrized and validated to support future development of different hardware configurations and advanced control strategies. The proposed models introduce a simulation framework for the development of improved solutions to optimize energy efficiency, reduce environmental emissions and increase user comfort.

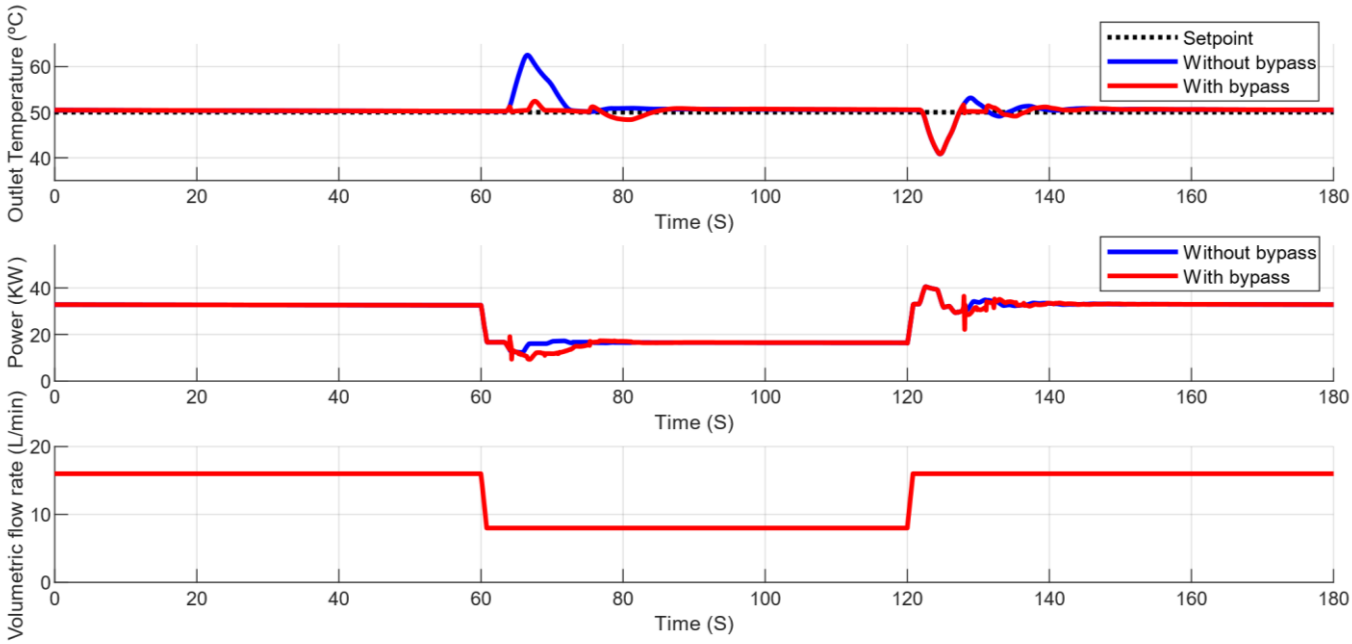

Figure 18: TGWH simulated thermostatic control, with and without bypass circuit.

A TGWH condensation appliance was selected for modelling, the heat cell was parametrized with experimental values and simulations were performed for typical flow rate changes that induced temperature overshoots and undershoots. Simulations results show that the proposed model effectively represents the dynamics of the selected appliance in different usage scenarios. The proposed TGWH individual components models enable the simulation of different hardware configurations, with or without bypass circuits, reservoir or mixing valves.

The proposed simulation platform allows the development of advanced control strategies in a simulated environment, taking advantage of the hardware in the loop techniques, without the need for a physical model and avoiding the associated safety risks.

The next task will be the research on the relationship between operation patterns and the level of pollutant gases emissions. Throughout laboratory tests, a qualitative model will be established and will be part of the model's library already developed.

Acknowledgements

The present study was developed in the scope of the **Smart Green Homes Project** [POCI-01-0247-FEDER-007678], a co-promotion between **Bosch Termotecnologia S.A.** and the **University of Aveiro**. It is financed by Portugal 2020 under the Competitiveness and Internationalization Operational Program and by the European Regional Development Fund.

References

[1] The Residential Energy Consumption Survey (RECS). Energy information administration official energy statistics from the US government, 2009.

[2] Eurostat European Commission, Energy, transport and environment indicators, Statistical Office of the European Union, 2017. doi:10.2785/964100.

[3] Commission regulation No. 814/2013 of 2 August 2013 implementing Directive 2009/125/EC of the European Parliament and of the Council with regard to ecodesign requirements for water heaters and hot water storage tanks, (2013).

[4] D. Bohac, B. Schoenbauer, M. Hewett, M.S. Lobenstein, T. Butcher, Actual savings and performance of natural gas tankless water heaters., in: ASHRAE Trans., Las vegas. NV, 2011.

[5] V. Costa, J. Ferreira, D. Guilherme, Modeling and simulation of tankless gas water heaters to reduce temperature overshoots and undershoots, in: 12th Int. Conf. Heat Transf. Fluid Mech. Thermodyn. (HEFAT 2016), Málaga, Spain, 2016: pp. 1404–1409.

[6] D.P. Yuill, A.H. Coward, G.P. Henze, Performance comparison of control methods for tankless water heaters, HVAC&R Res. 16 (2010) 677. doi:10.1080/10789669.2010.10390927.

[7] E.M.G. Rodrigues, R. Godina, E. Pouresmaeil, J.R. Ferreira, J.P.S. Catalão, Domestic appliances energy optimization with model predictive control, Energy Convers. Manag. 142 OP- (2017) 402. doi:10.1016/j.enconman.2017.03.061.

[8] S.A. Klein, TRNSYS 18: A Transient System Simulation Program, (2017). http://sel.me.wisc.edu/trnsys.

[9] G. Bourke, Integration of gas instantaneous auxiliaries with renewable energy residential water heaters, University of Auckland, 2015.

[10] J.B. Maguire, A Parametric Analysis of Residential Water Heaters, University of Colorado, 2012.

[11] J. Burch, M. Hoeschele, D. Springer, A. Rudd, Preliminary Modeling, Testing, and Analysis of a Gas Tankless Water Heater, in: SOLAR, National Renewable Energy Laboratory (U.S.), San Diego, California, 2008.

[12] J. Lutz, P. Grant, M. Kloss, Simulation Models for Improved Water Heating Systems, Project Report, 2013. doi:10.2172/1170604.

[13] G. Johnson, I. Beausoleil-Morrison, The calibration and validation of a model for predicting the performance of gas-fired tankless water heaters in domestic hot water applications, Appl. Energy. 177 (2016) 740. doi:10.1016/j.apenergy.2016.05.130.

[14] V. Gnielinski, New equations for heat and mass transfer in the turbulent flow in pipes and channels, Int. Chem. Eng. 16 (1976) 359–68.

[15] B. Petukhov, Heat Transfer and Friction in Turbulent Pipe Flow with Variable Physical Properties, Adv. Heat Transf. (1970).